Complex Berry phase dynamics in $\mathcal{PT}$-symmetric coupled waveguides

Rosie Hayward* and Fabio Biancalana

School of Engineering and Physical Sciences, Heriot-Watt University, EH14 4AS Edinburgh, United Kingdom

(Received 13 April 2018; revised manuscript received 24 August 2018; published 20 November 2018)

We show that the analog of the geometric phase for non-Hermitian coupled waveguides with $\mathcal{PT}$ symmetry and at least one periodically varying parameter can be purely imaginary, is hence no longer a true phase and instead a real multiplier, and will consequently result in the amplification of Floquet sidebands in the system. The sideband peaks seen in the spectrum of the system's eigenstates after evolution along the waveguides can be directly mapped to the spectrum of the derivative of the geometric function. The sidebands are magnified (becoming virtually unstable) as the exceptional point of the system is approached, and nonadiabatic effects begin to appear. Because the system cannot evolve adiabatically in the vicinity of the exceptional point, $\mathcal{PT}$ symmetry will be observed breaking earlier than theoretically predicted.

DOI: 10.1103/PhysRevA.98.053833

I. INTRODUCTION

Since the concept of a geometric phase in quantum mechanics was first described by Berry in 1984 [1], it has been extended such that it can be applied in many areas of physics, including to systems which are nonadiabatic and non-Hermitian [2,3]. As such, the effect it has on such systems is of considerable interest, in particular to the optics community. The analog of the Berry phase in a non-Hermitian system is easily derived via the traditional approach [4], through use of Floquet theorem [5,6], or by using an evolution operator method [7]. It is known that this geometric "phase" is not necessarily a real function for non-Hermitian systems, and hence it is possible for eigenstates to gain a real exponential multiplier, rather than simply a phase, after cyclic adiabatic evolution [2,7], leading to an exponential growth of the amplitude.

By replacing the requirement that a Hamiltonian be Hermitian with the weaker condition of parity-time ($\mathcal{PT}$) symmetry, a type of spacetime reflection symmetry, it is possible for it to have real eigenvalues as long as $\mathcal{PT}$ symmetry remains unbroken [8–10]. In the language of quantum mechanics, when $\mathcal{PT}$ symmetry is unbroken, the parity-time operator will commute with the Hamiltonian and share its instantaneous eigenstates; it breaks when the eigenstates of the Hamiltonian are no longer eigenstates of the $\mathcal{PT}$ operator [8]. Such non-Hermitian systems are easily realized in the field of optics; for example, as coupled waveguides with balanced gain and loss [11–14]. The $\mathcal{PT}$-symmetry-breaking point of such a system corresponds to an exceptional point in parameter space, where the eigenvalues and eigenstates of the system coalesce [11,15]. If the parameters cross this point, the eigenvalues of the system can become purely imaginary, and exponential gain will be observed in the waveguides.

Exceptional points have gained a lot of interest in recent years due to their various possible applications [15,16], and as such there have been interesting results concerning the geometric phase and the onset of instability in non-Hermitian systems. Theoretically, the adiabatic encircling of an exceptional point can lead to a state flip or the accumulation of a geometric phase in a two-level system [15]. However, in practice adiabaticity breaks down, as even with slow evolution the gain inherently present in such a system will magnify nonadiabatic effects which are usually neglected [17]. This is indeed what is observed in the work that follows. Furthermore, optical non-Hermitian systems near the exceptional point are known to be unstable with respect to infinitesimally small changes in the system's parameters [18].

In this work, we show that a non-Hermitian, $\mathcal{PT}$-symmetric coupled waveguide system with balanced gain and loss and a periodically varying coupling coefficient will have a purely imaginary geometric phase below the exceptional point. On approaching the exceptional point, adiabaticity will break down even for a slowly varying coupling between the waveguides, and it is consequently possible for the broken $\mathcal{PT}$-symmetry phase to occur earlier in parameter space than expected, due to the nonadiabatic "drift" of the energy eigenstates. It is, nevertheless, still possible to directly observe the contribution of the non-Hermitian geometric "phase" after cyclic evolution in the form of an amplification of the conventional Floquet sidebands appearing in Fourier space, due to the fact that the non-Hermiticity of the system allows the instantaneous eigenvectors to acquire an exponential change which no longer simply amounts to a phase factor. In principle, the appearance of such sidebands could be studied by using a Floquet theory adapted to non-Hermitian Hamiltonians (as was recently done in Ref. [19] in a similar system), however in this work we found much more useful to use a "Berry phase" approach, which gives a somewhat distinctive and interesting perspective on the phenomenon.

II. THE GEOMETRIC PHASE FOR NON-HERMITIAN SYSTEMS

Complex Hamiltonians, such as those containing gain and loss terms, will not in general be Hermitian, and will have a set of eigenvectors $|\psi_n(z)\rangle$ and adjoint eigenvectors $|\phi_n(z)\rangle$,

*Corresponding author: rh45@hw.ac.uk

such that

$$i\frac{d}{dz}|\psi_n(z)\rangle = \hat{H}(z)|\psi_n(z)\rangle, \tag{1}$$

and

$$i\frac{d}{dz}|\phi_n(z)\rangle = \hat{H}^\dagger(z)|\phi_n(z)\rangle, \tag{2}$$

which satisfy the following stationary equations:

$$\hat{H}(z)|\psi_n(z)\rangle = \lambda_n|\psi_n(z)\rangle, \tag{3}$$

and

$$\hat{H}^\dagger(z)|\phi_n(z)\rangle = \lambda_n^*|\phi_n(z)\rangle. \tag{4}$$

The eigenvectors and adjoint eigenvectors are bi-orthogonal and complete, such that $\langle\phi_m(z)|\psi_n(z)\rangle = 0$ for $m \neq n$, and the condition [20]

$$\sum_n \frac{|\psi_n(z)\rangle\langle\phi_n(z)|}{\langle\phi_n(z)|\psi_n(z)\rangle} = \hat{\mathbb{I}} \tag{5}$$

is satisfied, where $\hat{\mathbb{I}}$ is the identity operator.

Often in the literature, the normalization convention $\langle\phi_n(z)|\psi_n(z)\rangle = 1$ is enforced. However, normalizing the eigenvectors in this way when dealing with a system with exceptional or diabolical points can be problematic [15,21]. Although the inner products of states in quantum-mechanical Hermitian systems relate to probabilistic interpretations of measurement outcomes, the same interpretation cannot be applied to complex Hamiltonians [20]. As our system is optical, rather than quantum mechanical, and as one does not need to normalize the eigenvectors and adjoint eigenvectors to calculate the geometric phase, normalizing the states is unnecessary, and hence the convention is not enforced in this work.

For a general solution to the Schrödinger equation, $|\Psi(z)\rangle = \sum_n c_n(z)|\psi_n(z)\rangle e^{-i\int_0^z \lambda_n(z')dz'}$, we can solve to find the z evolution of the coefficients:

$$\left(\hat{H}(z) - i\frac{d}{dz}\right)|\Psi(z)\rangle = i\sum_n\left(\dot{c}_n|\psi_n\rangle + c_n\frac{d}{dz}|\psi_n\rangle\right) \times e^{-i\int_0^z \lambda_n(z')dz'} = 0. \tag{6}$$

Because we have a bi-orthogonal system, we take the inner product of the above with a particular adjoint eigenvector, $|\phi_n\rangle e^{-i\int_0^z \lambda_n^*(z')dz'}$, rather than an eigenvector, and find the condition

$$i\dot{c}_n\langle\phi_n|\psi_n\rangle = -c_n\left\langle\phi_n\left|i\frac{d}{dz}\right|\psi_n\right\rangle - c_m\left\langle\phi_n\left|i\frac{d}{dz}\right|\psi_m\right\rangle e^{-i\int_0^z[\lambda_n(z')-\lambda_m(z')]dz'}. \tag{7}$$

From here, if we assume the adiabatic approximation is upheld, we can neglect the c_m term above, since the oscillating phase will average out to zero in case of slow evolution, to get

$$\dot{c}_n = c_n i\frac{\langle\phi_n|i\frac{d}{dz}|\psi_n\rangle}{\langle\phi_n|\psi_n\rangle}, \tag{8}$$

which implies we can write the expansion coefficient c_n as an exponential phase factor, $e^{i\gamma_b(z)}$, and deduce that the geometric phase for our bi-orthogonal system is given by [4]

$$\gamma_b(z) = \int_0^z \frac{\langle\phi_n|i\frac{d}{dz'}|\psi_n\rangle}{\langle\phi_n|\psi_n\rangle}dz'. \tag{9}$$

Unlike the Berry phase, it is possible for the above to become purely imaginary, leading to eigenstates gaining a real, exponential multiplier during evolution. We shall see that the value of this real multiplier $e^{i\gamma_b(z)}$ is always positive when evolving along z, starts from zero, reaches a maximum, and comes back to zero after each cycle. This periodic multiplier can be associated with a Floquet–Bloch dynamics (see, for instance, the classical work [22]) and therefore will generate Floquet sidebands. Using Floquet–Bloch theory is definitely possible, however our approach based on the complex Berry phase is mathematically simpler (see, for instance, Ref. [23] for a recent example of the treatment of Floquet exceptional points) and we believe it is also physically more transparent—however, the two approaches must eventually lead to analogous if not identical results.

Of course we must also consider the secondary term in Eq. (7), proportional to the complex exponential, which can only be neglected for adiabatic evolution. In analogy with the standard procedure for Hermitian systems, we can assume the adiabatic approximation takes the form ($\hbar = 1$) [2,24]:

$$\left|\left\langle\phi_n\left|i\frac{d}{dz}\right|\psi_m\right\rangle\right| \ll |\lambda_m(z) - \lambda_n(z)|, \tag{10}$$

which can be rewritten in the following way:

$$\left|\frac{\langle\phi_n|i\frac{d\hat{H}(z)}{dz}|\psi_m\rangle}{\lambda_m(z) - \lambda_n(z)}\right| \ll |\lambda_m(z) - \lambda_n(z)|, \tag{11}$$

i.e., we require that the phase is evolving rapidly along z, and consequently the eigenvalue separation to be large, with respect to the change in z of the Hamiltonian.

The above condition should not be considered to always hold true in non-Hermitian systems, as they are known to exhibit quasi-adiabatic dynamical effects near exceptional points [25]. Consequently, even when the inequality (10) is upheld, we can expect that the instantaneous eigenstates may not evolve such that the final state of the system remains an instantaneous eigenstate, varying only by a complex phase factor.

III. $\mathcal{PT}$-SYMMETRIC COUPLED WAVEGUIDES WITH A PERIODIC COUPLING

A. Geometric phase

Consider $\mathcal{PT}$-symmetric linearly coupled waveguides with balanced gain and loss, as seen in Ref. [11], adapted so that the coupling between the waveguides varies periodically along the propagation direction z:

$$i\frac{d\psi_1}{dz} + \kappa(z)\psi_2 - i\gamma\psi_1 = 0, \tag{12a}$$

$$i\frac{d\psi_2}{dz} + \kappa(z)\psi_1 + i\gamma\psi_2 = 0, \tag{12b}$$

where ψ_1 and ψ_2 represent the modal field amplitude in each channel, respectively, $\kappa(z)$ is the periodically varying coupling coefficient between the waveguides, and γ is a scaled gain (loss) coefficient. Note that it is customary to use complex electric-field envelopes ψ_1 and ψ_2 to model light propagation in such systems, therefore avoiding the complications due to unnecessary presence of backward waves in Maxwell's equations.

This problem can be recast in the style of a quantum-mechanical two-level system with Hamiltonian

$$\hat{H} = \begin{pmatrix} i\gamma & -\kappa(z) \\ -\kappa(z) & -i\gamma \end{pmatrix}, \tag{13}$$

with instantaneous eigenvectors of the form

$$|\psi_n\rangle = \frac{1}{\sqrt{2}}\begin{pmatrix} \psi_1 \\ \psi_2 \end{pmatrix}.$$

It is easy to analytically solve the above. Making the substitution $\gamma/\kappa(z) = \sin[\alpha(z)]$, the eigenvectors can be concisely written as

$$|\psi_1\rangle = \frac{1}{\sqrt{2}}\begin{pmatrix} e^{-i\frac{\alpha}{2}} \\ e^{i\frac{\alpha}{2}} \end{pmatrix}, \quad |\psi_2\rangle = \frac{1}{\sqrt{2}}\begin{pmatrix} ie^{i\frac{\alpha}{2}} \\ -ie^{-i\frac{\alpha}{2}} \end{pmatrix}, \tag{14}$$

with corresponding eigenvalues

$$\lambda_1 = \lambda_2 = \mp\sqrt{\kappa^2(z) - \gamma^2}. \tag{15}$$

The adjoint eigenvectors can also be found by solving for the eigensystem of $\hat{H}^\dagger$:

$$|\phi_1\rangle = \frac{1}{\sqrt{2}}\begin{pmatrix} e^{i\frac{\alpha}{2}} \\ e^{-i\frac{\alpha}{2}} \end{pmatrix}, \quad |\phi_2\rangle = \frac{1}{\sqrt{2}}\begin{pmatrix} ie^{-i\frac{\alpha}{2}} \\ -ie^{i\frac{\alpha}{2}} \end{pmatrix}. \tag{16}$$

As the eigenvalues are real below the $\mathcal{PT}$ breaking point, the eigenvalues of the adjoint system are identical and real: $\lambda_1^* = \lambda_1$ and $\lambda_2^* = \lambda_2$.

It is easy to confirm that this system is $\mathcal{PT}$ symmetric because the Hamiltonian (13) commutes with the $\mathcal{PT}$ operator, as in Ref. [11]. In this case, the application of the $\mathcal{PT}$ operator corresponds to the transformation $\sigma_x \hat{H}^* \sigma_x$, where σ_x is the first Pauli matrix. This Hamiltonian can have an entirely real spectrum below the point where the system transitions to the broken $\mathcal{PT}$-symmetric phase. This point is crossed when the eigenvalues and eigenvectors coalesce, which in our case is when $\kappa(z) = \pm\gamma$ and $\lambda_1 = \lambda_2 = 0$. This is known as the *exceptional point* of the system [15].

For (assumed) adiabatic evolution of the eigenstates, we can find γ_b by using Eq. (9). In terms of α,

$$\gamma_b(z) = \frac{1}{2} i \ln\left[\frac{\cos[\alpha(z)]}{\cos[\alpha(0)]}\right]. \tag{17}$$

Substituting $\cos[\alpha(z)] = [1 - \gamma^2/\kappa^2(z)]^{1/2}$, we find

$$\gamma_b(z) = \frac{1}{2} i \ln\left[\frac{\sqrt{1 - \gamma^2/\kappa^2(z)}}{\sqrt{1 - \gamma^2/\kappa^2(0)}}\right], \tag{18}$$

which is clearly a purely imaginary function below the $\mathcal{PT}$-symmetry-breaking point $\kappa(z) = \pm\gamma$, which must be upheld for all z. As a consequence of this, eigenstates no longer gain a phase factor on evolution, but are multiplied by a real, periodic function: $e^{i\gamma_b(z)}$. Despite the fact that the Berry phase $\gamma_b(z)$ becomes purely imaginary and is thus no longer a phase but a geometric multiplier, the formula used to find it is the original non-Hermitian Berry phase formula, which in general corresponds to complex phases [4]. This should not create a confusion when we refer to it as a Berry phase, keeping in mind that the argument of the exponential becomes purely real.

One is able to see evidence of this function's influence when examining the spectrum of our system's instantaneous eigenstates after allowing them to evolve along a waveguide of length L, in the form of existing Floquet sidebands increasing in amplitude due to the non-Hermitian nature of the Hamiltonian. Ultimately, the position of the spectral sidebands in Fourier space can be traced to the deformations of the "instantaneous wave number" [$\equiv\gamma_b'(z)$], similar to what happens in nonlinear systems, although Eqs. (12) are of course fully linear; the non-Hermitian Hamiltonian (13) is nonconservative and gives rise to the amplification of such sidebands.

As we previously mentioned, the same sidebands could in principle be found by using a Floquet–Bloch approach [22,23,26,27]: if gain and losses are removed from the system ($\gamma = 0$), and we simply have a periodic modulation of the coupling coefficient, then indeed Floquet peaks will be seen in the spectrum of the eigenstates after evolution (since the eigenstates will acquire a nontrivial z-dependent phase that will affect the resulting spectrum), and the geometric function given by Eq. (9) will be zero. However, when gain and losses are present ($\gamma \neq 0$), the complex Berry phase formalism is able to capture not only the formation and further amplification of the Floquet sidebands, but also quite easily capture the mixing between the two eigenstates, especially when the parameters approach the exceptional point of the system—this mixing is quantified by the breaking of adiabaticity of Eq. (10). We shall explore this issue in the next section.

In the results which follow, we choose, as a representative example, the following periodic evolution for the coupling coefficient:

$$\kappa(z) = 1 - a + a\cos(k_0 z), \tag{19}$$

where a (the depth of the modulation) and $k_0 \equiv 2\pi/\Lambda$ (the wave number of the modulation, proportional to the inverse of the modulation period) are real, positive parameters. Waveguides with harmonic behavior in the coupling, such as that seen in Eq. (19), can be easily made with current technology by combining two waveguides of the type fabricated in, for instance, Ref. [28]. It is easy to see that the minimum value of this function is $1 - 2a$, which allows us to find a minimum threshold at which $\mathcal{PT}$ symmetry will break in terms of the parameter a:

$$a = \frac{1 - \gamma}{2}. \tag{20}$$

Of course, this is based on the assumption that the adiabatic condition is upheld. If, as can be expected for a nonadiabatically evolving system, the eigenstates do not remain in their instantaneous forms, then of course we cannot as easily predict the point in parameter space where they will coalesce.

B. Nonadiabatic evolution

For a periodic coupling $\kappa(z)$ which changes too rapidly in z, we can expect that requirement (10) will not be fulfilled.

In this case, the eigenvalues of the system will drift from those corresponding to the instantaneous eigenstates, which will consequently change the expected $\mathcal{PT}$-symmetry-breaking point. For our system, the condition for adiabatic evolution takes the form

$$\left|\frac{1}{2}\frac{\gamma\kappa'(z)}{\kappa^2(z)-\gamma^2}\right| \ll \left|2\sqrt{\kappa^2(z)-\gamma^2}\right|, \tag{21}$$

where $\kappa'(z)$ is the z derivative of the coupling coefficient $\kappa(z)$. This can be conveniently rearranged to place a constraint on $\kappa'(z)$, allowing us to determine whether the system is likely to be evolving adiabatically based on its rate of change:

$$\left|\frac{d}{dz}\kappa(z)\right| \ll \left|\frac{4}{\gamma}[\kappa^2(z)-\gamma^2]^{3/2}\right|. \tag{22}$$

Even for a slowly varying coupling $\kappa(z)$, characterized by a small value of k_0, because our system is non-Hermitian we can expect it to display nonadiabatic behavior as we approach the exceptional point [17]. Hence, changing k_0 will only make significant difference in whether the system appears to be evolving adiabatically for small values of a. If a is too close to the value given by Eq. (20), the value of k_0 is irrelevant.

It is worth mentioning at this stage that a nonadiabatic generalization of the Berry phase was introduced for cyclic Hamiltonians by Aharonov and Anandan [3] and extended to dissipative systems by Garrison and Wright [2]. In the vicinity of degeneracies related to exceptional or diabolical points, where condition (10) is violated, one can instead use the definition given in Ref. [24]. However, in this work, we will continue to use the definition given by Berry for non-Hermitian systems, seen in Eq. (9), because it does not require the system to be bi-orthonormal (which is violated at exceptional points), and should still be observable, even if there are additional effects due to nonadiabatic behavior present in the results.

IV. FORMATION AND NON-HERMITIAN AMPLIFICATION OF SIDEBANDS

We now present results of numerical simulations of Eqs. (12), solved with a fourth-order Runge–Kutta algorithm, which demonstrate that the growth and amplification of Floquet-like sidebands in the spectrum of states evolved along the coupled waveguides is due to the imaginary geometric function given by Eq. (18). The geometric function $i\gamma_b(z)$, as given by Eq. (18), and its derivative $i\gamma_b'(z)$ are shown in Figs. 1(a) and 1(b), respectively, for $\gamma = 0.5$, $k_0 = 1$, and $a = 0.2$. The deformed appearance of $i\gamma_b'(z)$ increases with increasing values of the parameter a, as does the amplitude of both functions, and both functions will become singular at the exceptional point of the system, $a = 0.25$, which can be found using Eq. (20).

In our simulation, if a superposition of both eigenstates $|\psi_1\rangle + |\psi_2\rangle$ is initially excited and then propagated along the coupled waveguides described by Eqs. (12a) and (12b) for a waveguide distance $L = 1000$, then for $a = 0$ one will see two peaks in Fourier space, as seen in Fig. 2. Both eigenstates remain in their instantaneous forms, as should be expected for a constant coupling constant κ. The positive peak corresponds to $|\psi_1\rangle$ and the negative to $|\psi_2\rangle$, and we shall label them k_1 and k_2, respectively. In z space, if only $|\psi_1\rangle$ or $|\psi_2\rangle$ is excited, then there will be no oscillation. If we excite the superposition, then there will be a visible oscillation in z space due to the beating frequency created by the presence of k_1 and k_2. Consequently, the oscillation period in z will be given by $2\pi/(k_1 - k_2)$.

Figure 3(a) shows the logarithmic spectrum seen after propagation along the coupled waveguides of $L = 1000$ when exciting a superposition of both eigenstates for $a = 0.15$, $k_0 = 1$, and $\gamma = 0.5$. The two highest peaks correspond to k_1 and k_2, and as predicted in the previous sections we also see

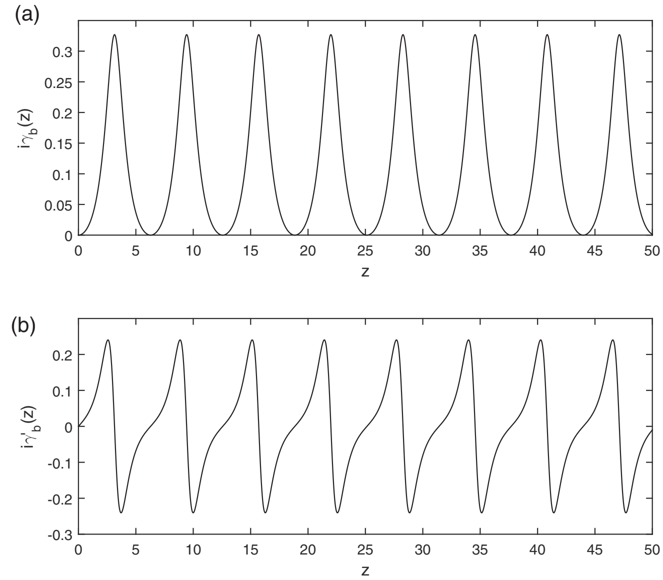

FIG. 1. (a) Plot of $i\gamma_b(z)$, as given by Eq. (18), and (b) its z derivative. In both cases $k_0 = 1$, $a = 0.22$, and $\gamma = 0.5$. For increasing values of a, the amplitude of $i\gamma_b(z)$ and $i\gamma_b'(z)$ will increase, and $i\gamma_b'(z)$ will become increasingly deformed. Both functions become singular at $a = 0.25$, which is the exceptional point of the system when $\gamma = 0.5$, as given by Eq. (20).

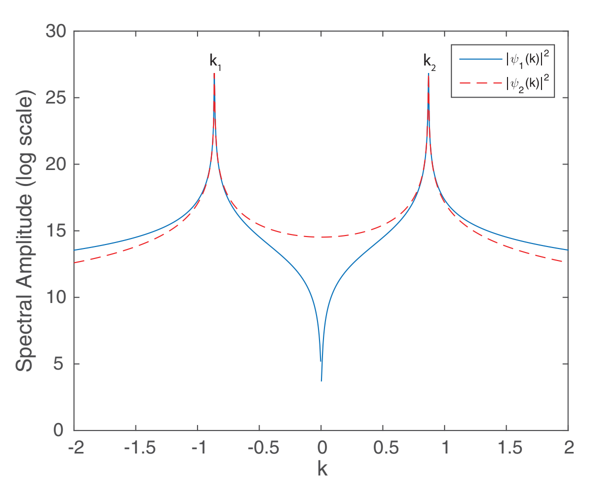

FIG. 2. Plot of the logarithmic spectrum of the waveguide modes ψ_1 and ψ_2, when both eigenstates are excited in a superposition $|\psi_1\rangle + |\psi_2\rangle$, and $a = 0$. The right-hand peak corresponds to $|\psi_1\rangle$ and the left to $|\psi_2\rangle$, and we can label them k_1 and k_2, respectively.

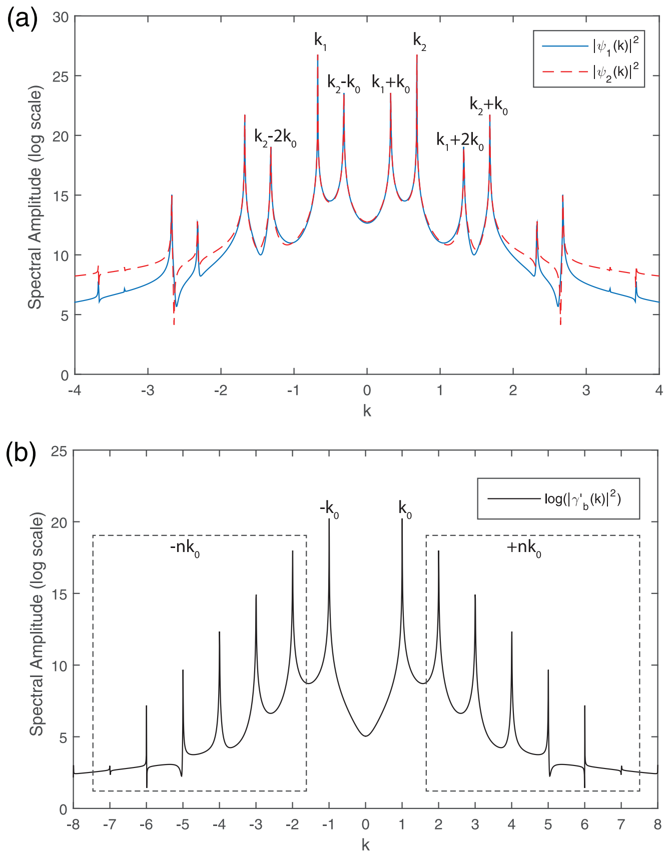

FIG. 3. (a) The spectrum seen when the initial state of the system is input as $|\psi_1\rangle + |\psi_2\rangle$ for $a = 0.15$, $k_0 = 1$, and $\gamma = 0.5$. The two highest peaks correspond to k_1 and k_2, although the separation between the two has decreased in comparison with Fig. 2. (b) The spectrum of the function $i\gamma_b'(z)$, as seen in Fig. 1. The peaks are found at $\pm nk_0$, where n is a nonzero integer. Despite the fact $a = 0.15$ is not very close to the exceptional point of the system, the new peaks have a very strong presence. They can be found at $k_1 \pm nk_0$ and $k_2 \pm nk_0$, suggesting the geometric multiplier is the source of the magnification of the sidebands, as predicted.

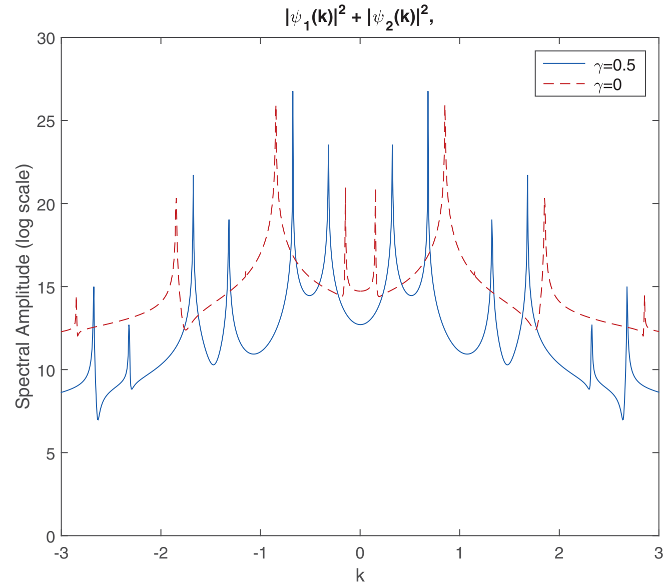

FIG. 4. Spectra (on a logarithmic scale) of the evolved states of the coupled waveguide system in the Hermitian case ($\gamma = 0$, red dashed line) and the non-Hermitian one ($\gamma = 0.5$, blue solid line), both calculated for $a = 0.15$ and a propagation length of $L = 1000$. This shows that the Floquet peaks coming from the periodic modulation of the coupling constant are shifted and amplified due to the introduction of the non-Hermitian factor γ.

the appearance of sidebands. In Fig. 3(b) we can clearly see that the peaks correspond to the points $\pm nk_0$ in Fourier space, where $n \in \mathbb{N}$. As a result, the peaks in Fig. 3(a) correspond to k values of $k_1 \pm nk_0$ and $k_2 \pm nk_0$. In comparison with Fig. 2, the separation between k_1 and k_2 has decreased. This is in line with the expectation that the two instantaneous eigenstates of the system will approach each other as the exceptional point is approached.

In Fig. 4 we show the comparison between a Hermitian propagation ($\gamma = 0$, red dashed line) and a non-Hermitian one ($\gamma \neq 0$, blue solid line). This comparison shows that we are still dealing with two sets of equally spaced Floquet peaks, emerging from the periodic modulation of the coupling constant κ, but in the latter case the non-Hermitian Berry "phase" introduces an amplification of the Floquet sidebands, which is encoded in the single "complex Berry phase" framework expressed by Eq. (9).

In Fig. 5, the z-space oscillations and corresponding spectrum at $L = 1000$ is seen when only $|\psi_1\rangle$ is excited for $a = 0.1$. Because a is fairly small and reasonably far from the exceptional point ($a = 0.25$), the influence of the peaks is not as strong as that seen in Fig. 3. Furthermore, because only $|\psi_1\rangle$ is initially excited, the spectrum is asymmetric. Nevertheless, the presence of the k_2 peak is clear, although it is not as strong as the peak k_1, and could be easily mistaken for a Berry phase peak. Its appearance suggests that the system is not evolving adiabatically, which is to be expected when examining the inequality (22): as a grows the $\kappa(z)$ derivative will gradually become comparable in magnitude with the inequality's right-hand side. Examining the z evolution of $|\psi_1|^2$ and $|\psi_2|^2$ in Fig. 5(a) will again reveal the appearance of oscillations due to the simultaneous presence of k_1 and k_2. These appear similar to the oscillations seen in Ref. [29], known as Rabi oscillations, where gain and loss, rather than the coupling, are driven. It should be noted that, unlike those seen in Ref. [29], the oscillations of $|\psi_1|^2$ and $|\psi_2|^2$ are not perfectly out of phase, and also appear to show some deformation, suggesting they are being influenced by $i\gamma_b'(z)$, as seen in Fig. 1(b).

As a is increased, a strong beating in z space will appear, and despite exciting only one eigenstate initially, both k_1 and k_2 will appear in the spectrum with equal strength, displaying a complete breakdown of adiabatic evolution. This is shown in Fig. 6 for $a = 0.22$, $k_0 = 1$, and $\gamma = 0.5$, where again only $|\psi_1\rangle$ has been initially excited. The envelope of the smaller oscillations observed is characteristic of the $\mathcal{PT}$-symmetry-breaking point being approached, and the amplitude of this envelope will grow for increasing values of the parameter a. Furthermore, one should note that, due to the decrease in the separation between k_1 and k_2, the peaks have moved much closer to one another and are approaching the point of overlap. The separation between the maxima of the envelope wave

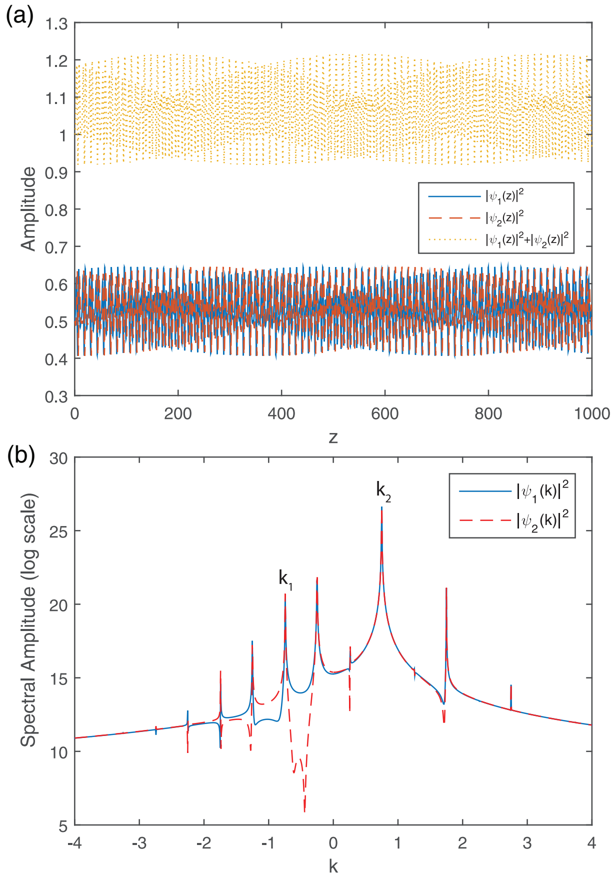

FIG. 5. (a) Evolution in z when the initial state is the instantaneous eigenstate $|\psi_1(0)\rangle$ for $a = 0.1$, $k_0 = 1$, and $\gamma = 0.5$ of $|\psi_1|^2$ (blue solid line), $|\psi_2|^2$ (red dashed line), and their sum, equivalent to the norm squared of the evolved eigenstate $|\langle\psi_1(z)|\psi_1(z)\rangle|^2$ (yellow dotted line). The oscillations in z space are periodic, but also deformed, displaying evidence of the influence of multiple frequencies and the presence of the geometric multiplier $e^{i\gamma_b(z)}$. (b) The logarithmic spectrum is taken at $L = 1000$ corresponding to the data shown in panel (a). The spectrum no longer displays the symmetry seen before, due to the fact only a single eigenstate is excited. Nevertheless, a smaller peak corresponding to k_2 is present, suggesting a departure from adiabatic evolution, as well as the majority of the expected sidebands.

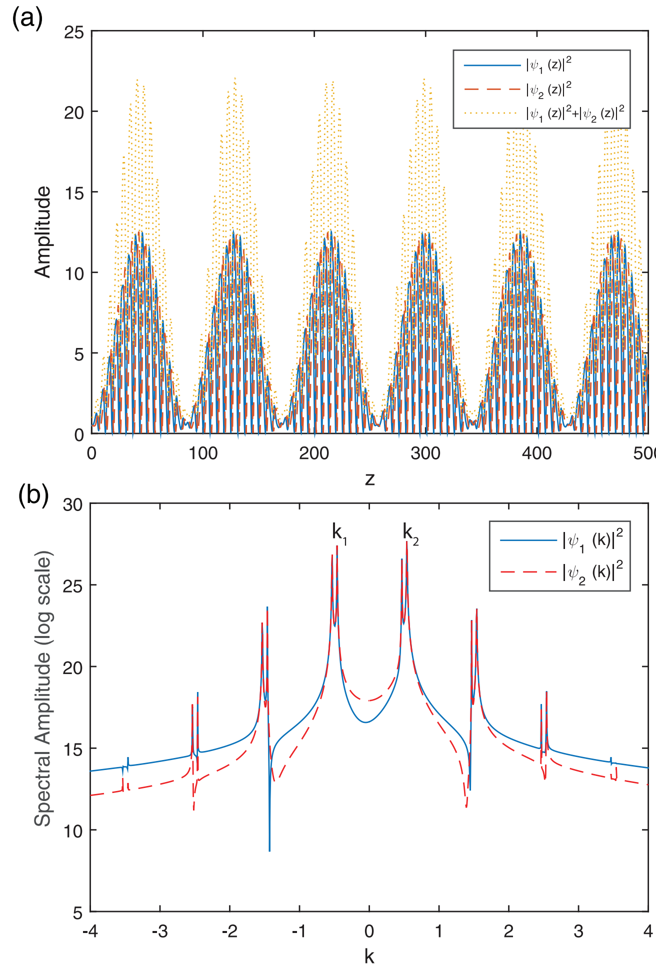

FIG. 6. (a) Evolution in z when the initial state is the instantaneous eigenstate $|\psi_1(0)\rangle$ for $a = 0.22$, $k_0 = 1$, and $\gamma = 0.5$ of $|\psi_1|^2$ (blue solid line), $|\psi_2|^2$ (red dashed line), and their sum, equivalent to the norm squared of the evolved eigenstate $|\langle\psi_1(z)|\psi_1(z)\rangle|^2$ (yellow dotted line). The oscillations in z space are still present, and a clear beating enveloping the smaller oscillations has appeared. (b) The spectrum taken at $L = 1000$ corresponding to the data shown in panel (a). The logarithmic spectrum is now symmetric, despite no initial excitation of $|\psi_2\rangle$, which implies a complete departure from adiabatic behavior. The separation between all peaks has decreased, and the smallest separation between peaks can be directly linked to the beating seen in z space, as explained in the main text.

observed in z space can be shown to be approximately equal to 2π divided by the smallest separation of peaks in the spectrum, e.g., the separation between two peaks in Fourier space.

In the simulation, the $\mathcal{PT}$ symmetry of the system breaks at approximately $a = 0.223$ for $\gamma = 0.5$ and $k_0 = 1$. This is characterized by the onset of exponential gain in z space, suggesting the exceptional point of the system has been crossed and the energies of $|\psi_1\rangle$ and $|\psi_2\rangle$ have become imaginary. The evolution of the system after this point is crossed can be seen in Fig. 7(a), with the corresponding spectrum shown in Fig. 7(b), for $a = 0.225$, $\gamma = 0.5$, and $k_0 = 1$. The early onset of the broken $\mathcal{PT}$-symmetry phase (compared with the theoretically predicted break point of $a = 0.25$) should not be surprising given the clearly nonadiabatic behavior of the system; the drift of $|\psi_1\rangle$ and $|\psi_2\rangle$ from their instantaneous forms makes the precise point at which they will coalesce very difficult to predict with the estimates we give in previous sections. In Fig. 7(b) we can see that the sidebands have now overlapped, and the separation between k_1 and k_2 has reduced, such that it is equal to the parameter k_0. This is not a coincidence—changing k_0 will determine the peak separation at the $\mathcal{PT}$-symmetry-breaking point observed in the simulation.

In the results so far we have only seen the behavior of our coupled waveguide system for $k_0 = 1$, which can be freely chosen. It may seem that, by reducing this value, one can better ensure that the inequality (22) is upheld, and likewise by increasing it ensure the opposite, enabling one to find a case where the system displays $\mathcal{PT}$ symmetry breaking at the expected point of $a = 0.25$, in a similar vein to what is seen

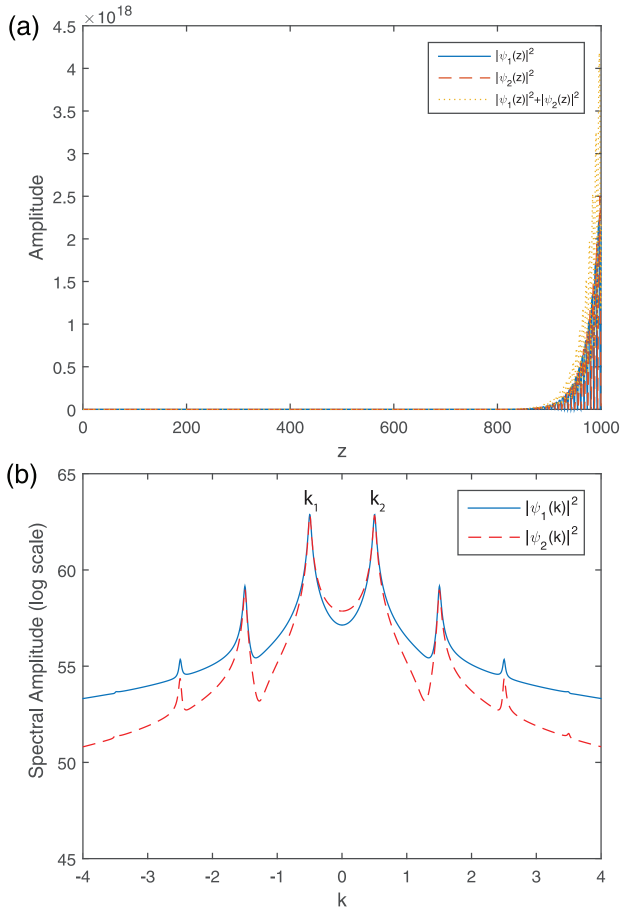

FIG. 7. (a) Evolution in z when the initial state is the instantaneous eigenstate $|\psi_1(0)\rangle$ for $a = 0.225$, $k_0 = 1$, and $\gamma = 0.5$ of $|\psi_1|^2$ (blue solid line), $|\psi_2|^2$ (red dashed line), and their sum, equivalent to the norm squared of the evolved eigenstate $|\langle\psi_1(z)|\psi_1(z)\rangle|^2$ (yellow dotted line). There is clear exponential gain, suggesting $\mathcal{PT}$ symmetry has been broken and the energies of the system have become imaginary. (b) The logarithmic spectrum taken at $L = 1000$ corresponding to the data shown in panel (a). The separation between the two central peaks is now equal to k_0, and the previously approaching peaks have now overlapped.

in Ref. [30]. However, in practice this does not work: close to the exceptional point, no matter how slow the variation of the coupling is in z, the system will not behave adiabatically, making it very difficult to predict accurately where the $\mathcal{PT}$ symmetry will break in the simulation. This is in line with what is already known about non-Hermitian systems, as reported in Ref. [17], where it is shown that the gain inherently present in non-Hermitian systems will magnify usually-neglected adiabatic effects.

V. CONCLUSIONS

It is shown that the eigenstates of a non-Hermitian, $\mathcal{PT}$-symmetric coupled waveguide system with a periodically varying coupling will gain a purely imaginary geometric multiplier on evolution, which will in turn induce the non-Hermitian amplification of Floquet sidebands in the system, visible in the spectrum of the evolved eigenstates. The magnitude of the growth increases as the system approaches its $\mathcal{PT}$-symmetry-breaking point, which is observed to break for a smaller value of the parameter a than theoretically predicted. This is expected, because the conditions required for adiabatic evolution in non-Hermitian systems is violated in the vicinity of the exceptional point. Beyond the $\mathcal{PT}$-symmetry-breaking point, exponential gain will be observed in the coupled waveguides. This mechanism of sideband growth has interesting implications for the optics community. Learning how to control the output of a waveguide system by modulating the distance between the waveguides (and thus modulating the coupling) could lead to new switching or routing devices based on the complex Berry phase [31]. Furthermore, it is possible that such amplification of sidebands will also be visible in other branches of physics in which non-Hermitian two-level systems can be found, such as photon fluids, where complex Berry phases are also known to arise [32].

ACKNOWLEDGMENT

The authors would like to acknowledge funding from the EPSRC CM-CDT Grant No. EP/L015110/1.

[1] M. V. Berry, Proc. R. Soc. London, Ser. A **392**, 45 (1984).
[2] J. C. Garrison and E. M. Wright, Phys. Lett. A **128**, 177 (1988).
[3] Y. Aharonov and J. Anandan, Phys. Rev. Lett. **58**, 1593 (1987).
[4] M. Berry, Ann. N. Y. Acad. Sci. **755**, 303 (1995).
[5] H. Choutri, M. Maamache, and S. Menouar, J. Korean Phys. Soc. **40**, 358 (2002).
[6] M. Maamache, Phys. Rev. A **92**, 032106 (2015).
[7] G. Dattoli *et al.*, J. Phys. A: Math. Gen. **23**, 5795 (1990).
[8] C. M. Bender, Contemp. Phys. **46**, 277 (2005).
[9] C. M. Bender and S. Boettcher, Phys. Rev. Lett. **80**, 5243 (1998).
[10] C. M. Bender, M. V. Berry, and A. Mandilara, J. Phys. A: Math. Gen. **35** L467 (2002).
[11] H. Ramezani, T. Kottos, R. El-Ganainy, and D. N. Christodoulides, Phys. Rev. A **82**, 043803 (2010).
[12] R. El-Ganainy, K. G. Makris, D. N. Christodoulides, and Z. H. Musslimani, Opt. Lett. **32**, 2632 (2007).
[13] A. Guo, G. J. Salamo, D. Duchesne, R. Morandotti, M. Volatier-Ravat, V. Aimez, G. A. Siviloglou, and D. N. Christodoulides, Phys. Rev. Lett. **103**, 093902 (2009).
[14] C. E. Rüter *et al.*, Nat. Phys. **6**, 192 (2010).
[15] J. Doppler, A. A. Mailybaev, J. Bohm, U. Kuhl, A. Girschik, F. Libisch, and S. Rotter, Nature (London) **537**, 76 (2016).
[16] H. Ramezani, T. Kottos, V. Kovanis, and D. N. Christodoulides, Phys. Rev. A **85**, 013818 (2012).
[17] R. Uzdin, A. Mailybaev, and N. Moiseyev, J. Phys. A: Math. Theor. **44**, 435302 (2011).
[18] A. A. Zyablovsky, E. S. Andrianov, and A. A. Pukhov, Sci. Rep. **6**, 29709 (2016).
[19] Y. Wu *et al.*, Front. Phys. **12**, 121102 (2017).
[20] D. Brody, J. Phys. A: Math. Theor. **47**, 035305 (2014).

[21] F. Keck, H. J. Korsch, and S. Mossmann, J. Phys. A: Math. Gen. **36**, 2125 (2003).
[22] S. Trillo and S. Wabnitz, Phys. Rev. E **56**, 1048 (1997).
[23] S. Longhi, J. Phys. A: Math. Theor. **50**, 505201 (2017).
[24] A. I. Nesterov and F. Aceves de la Cruz, J. Phys. A: Math. Theor. **41**, 485304 (2008).
[25] T. J. Milburn, J. Doppler, C. A. Holmes, S. Portolan, S. Rotter, and P. Rabl, Phys. Rev. A **92**, 052124 (2015).
[26] L. D. Landau and E. M. Lifshitz, *Mechanics and Electrodynamics* (Pergamon Press Ltd., Oxford, 1972).
[27] V. I. Arnol'd, *Mathematical Methods of Classical Mechanics*, in Graduate Texts in Mathematics (Springer, New York, 1989).
[28] T. Eichelkraut *et al.*, Opt. Lett. **39**, 6831 (2014).
[29] T. E. Lee and Y. N. Joglekar, Phys. Rev. A **92**, 042103 (2015).
[30] A. Jaouadi *et al.*, J. Phys. B: At., Mol. Opt. Phys. **46**, 145402 (2013).
[31] A. Lupu, H. Benisty, and A. Degiron, Photonics Nanostruct. **12**, 305 (2014).
[32] N. Westerberg, C. Maitland, D. Faccio, K. Wilson, P. Ohberg, and E. M. Wright, Phys. Rev. A **94**, 023805 (2016).